

# Superinfections and adaptive dynamics of pathogen virulence revisited: a critical function analysis

Barbara Boldin, Stefan A.H. Geritz and Éva Kisdi

*Department of Mathematics and Statistics, University of Helsinki, Helsinki, Finland*

---

## ABSTRACT

**Background:** Superinfections are known to facilitate the co-existence of several pathogen strains in a host population. Previous models have demonstrated that pathogen virulence may undergo evolutionary branching, whereby an ancestral strain splits into two strains of different virulence. Evolutionary branching depends on the superinfection function as well as the trade-off between virulence and transmission, but reliable empirical data for these functions are scarce.

**Aim:** To find necessary and sufficient conditions for evolutionary branching in an SI model (where S stands for susceptible and I for infected/infectious) with superinfections under any conceivable transmission–virulence trade-off.

**Methods:** Adaptive dynamics and critical function analysis.

**Assumptions:** The superinfection function is assumed to be differentiable, but otherwise arbitrary. We consider three different modes of host population dynamics: constant population size, constant population birth rate, and logistic population growth in the absence of pathogens.

**Results:** In the constant population birth rate model, evolutionary branching can always occur if the convexity of the trade-off falls in a certain range; this range can however be narrow, especially if the singularity is at high virulence and relatively low transmission. With constant population size and with logistic growth, mutual exclusion of strains occurs near some singularities, which excludes evolutionary branching in part of the parameter space.

**Comparison of methods:** We show how critical function analysis relates to a more traditional analysis of the model via pairwise invasibility plots and bifurcation plots of evolutionary singularities.

*Keywords:* adaptive dynamics, co-existence of pathogen strains, critical function analysis, evolutionary branching, superinfection model, trade-off, virulence evolution.

## INTRODUCTION

In superinfection models, it is generally assumed that a more virulent strain can infect a host individual previously infected with a less virulent strain, whereupon the less virulent strain is cleared from the host and the individual is taken over by the more virulent infection. Superinfections explain the co-existence of different pathogen strains in a homogeneous

---

Correspondence: É. Kisdi, Department of Mathematics and Statistics, University of Helsinki, PO Box 68, FIN-00014 Helsinki, Finland. e-mail: eva.kisdi@helsinki.fi

Consult the copyright statement on the inside front cover for non-commercial copying policies.

---

host population (Levin and Pimentel, 1981; Nowak and May, 1994; Castillo-Chavez and Velasco-Hernandez, 1998; Mosquera and Adler, 1998). More virulent strains enjoy an advantage by being able to infect more host individuals (i.e. susceptible hosts *and* hosts infected with less virulent strains); however, they also suffer a disadvantage, as they kill their hosts faster and hence have less time to infect new hosts. As noted by May and Nowak (1994), co-existence of pathogen strains by superinfections is similar in many aspects to co-existence of competing species by the competition–colonization trade-off (Levins and Culver, 1971; Nee and May, 1992; Tilman, 1994; Geritz, 1995), where one species competitively displaces the other within a habitat patch (such as a host) but produces less colonizers or has a higher rate of local extinction (host death).

Superinfection models can also explain the evolutionary origin of co-existing pathogen strains. Adler and Mosquera-Losada (2002) and Boldin and Diekmann (2008) reported evolutionary branching under superinfection, whereby the pathogen population gradually splits into two co-existing strains with increasingly different virulence. This is again broadly paralleled by evolutionary branching under the competition–colonization trade-off, such as evolutionary branching of seed size when size amounts to competitive advantage but size is traded off against the number of colonizing offspring (Geritz *et al.*, 1999). Both the co-existence of pathogen strains under superinfections and co-existence by the competition–colonization trade-off may be viewed as instances of asymmetric competition, where *relative* competitive advantage (i.e. virulence higher than that of the existing infection, or seed size larger than that of the competitors) can be bought at an *absolute* cost (death of the host, low number of seeds) incurred also in the absence of competition (when infecting a host free of any pathogen or a single seed colonizing a patch of habitat). In addition to driving evolutionary arms races (Parker, 1983; Maynard Smith and Brown, 1986; Matsuda and Abrams, 1994), asymmetric competition in general facilitates evolutionarily stable co-existence (Abrams and Matsuda, 1994) and evolutionary branching (Kisdi, 1999; Kisdi and Geritz, 2001).

In this paper, we specifically search for conditions leading to evolutionary branching of a pathogen in the simplest superinfection model. The model has two important functions that determine its behaviour: the superinfection function and the transmission–virulence trade-off.

The superinfection function gives the probability that a host individual already infected by a strain of the pathogen can be taken over by a new infection. Superinfections by more virulent strains are mechanistically explained by the within-host dynamics of competing pathogen strains assuming fast dynamics within a host and the absence of cross-immunity (Boldin and Diekmann, 2008). If the only interaction between pathogens within a single host individual is competition for host resources, and the more virulent strain equilibrates host resources at a lower level than the less virulent strain, then within-host competitive exclusion leads to the establishment of the more virulent strain and loss of the less virulent infection. However, given that only a limited number of bacteria or viruses of the superinfecting strain enter the host body, the within-host dynamics of the superinfection is initially subject to demographic stochasticity, and hence a more virulent strain takes the host over only with a certain (positive) probability (Jagers, 1975; Boldin and Diekmann, 2008). This probability,  $\rho(\alpha_2 - \alpha_1)$ , is an increasing function of the difference between the virulence of the superinfecting strain ( $\alpha_2$ ) and that of the existing infection ( $\alpha_1$ ). We refer to  $\rho(\alpha_2 - \alpha_1)$  as the superinfection function. Because we assume mutations of small effect and concentrate on evolution in essentially monomorphic populations (including incipient evolutionary branching), it is sufficient to know the behaviour of  $\rho$  in the vicinity of zero; more precisely, it is sufficient to know the value  $\rho(0)$  and the derivative  $\rho'(0)$ , which we can treat as

two parameter values of the model. The global shape of  $\rho(\alpha_2 - \alpha_1)$  plays a role in the co-evolution of two or more strains with significantly different virulences.

Virulence affects not only the probability of superinfection but also the transmission rate of the pathogen. More virulent strains maintain higher pathogen concentration within the host, and may produce more severe symptoms (such as coughing, bleeding, etc.) that enhance the transmission of the pathogen to a new host individual. Indeed, the shape of the trade-off between increased transmission (benefit) and increased virulence (cost due to host death) is critical to the outcome of pathogen evolution (Pugliese, 2002; Svernungsen and Kisdi, in press; see also Ganusov and Antia, 2003). Measuring the shape of this trade-off is difficult, so we have no reliable empirical data that can be used to support a particular choice of the trade-off function.

The unknown transmission–virulence trade-off may be derived from an underlying model of the within-host infection process (e.g. Gilchrist and Sasaki, 2002; Alizon and van Baalen, 2005; Boldin and Diekmann, 2008; for a review, see Mideo *et al.*, 2008). Alternatively, one can turn the question around and ask what the trade-off function should look like to obtain a certain evolutionary outcome [e.g. an evolutionarily stable strategy (ESS) or evolutionary branching of the pathogen at a given point]; or, indeed, whether a certain outcome is possible at all under any conceivable trade-off. In this paper, we take this second route and use the technique called ‘critical function analysis’ to explore the possible evolutionary scenarios under any trade-off (de Mazancourt and Diekmann, 2004; Kisdi, 2006; Geritz *et al.*, 2007; Svernungsen and Kisdi, in press; for a related approach, see Bowers *et al.*, 2005).

In the superinfection model we revisit, Adler and Mosquera Losada (2002) found evolutionary branching using one simple function for the transmission–virulence trade-off. Pugliese (2002), on the other hand, proved that evolutionary branching cannot occur and evolution leads to an ESS for a class of concave trade-off functions. Our critical function analysis reveals necessary and sufficient conditions for evolutionary branching as well as for convergence stable (attracting) ESSs and evolutionary repellors. Since previous studies made different assumptions about the population dynamics of the host, we perform critical function analysis under three different modes of host density regulation (constant population size, constant population birth rate, and logistic population growth). In the second part of the paper, we illustrate the results with examples of adaptive dynamics of virulence given a certain trade-off function, and a traditional bifurcation analysis of the evolutionary dynamics given a parameterized family of trade-off functions.

## THE MODEL

We consider a simple SI model (where S stands for susceptible and I for infected/infectious), thereby focusing on chronic pathogens with no recovery. Let the population density of susceptibles be  $S$ , and let the density of hosts infected with pathogen strain 1, . . . ,  $k$  be  $I_1, \dots, I_k$ ; we denote the total population density by  $N$ ,  $N = S + \sum_{i=1}^k I_i$ . The population dynamics are given by

$$\frac{dS}{dt} = b(N)N - \sum_i \beta(\alpha_i)I_i S - \mu S \quad (1a)$$

$$\frac{dI_i}{dt} = \left[ \beta(\alpha_i)S + \sum_j \beta(\alpha_i) \rho(\alpha_i - \alpha_j)I_j - \sum_j \beta(\alpha_j) \rho(\alpha_j - \alpha_i)I_j - \alpha_i - \mu \right] I_i \quad (1b)$$

for  $i = 1, \dots, k$ . All newborns are susceptible, and the host population is regulated by a density-dependent per capita birth rate,  $b(N)$ . The natural death rate is  $\mu$ . Hosts infected with strain  $i$  suffer disease-related death at rate  $\alpha_i$ , the virulence of the pathogen. Infections follow mass action, where the transmission rate of strain  $i$ ,  $\beta(\alpha_i)$ , depends on its virulence according to the transmission–virulence trade-off. For the critical function analysis we do not assume any particular trade-off function, but for simplicity of the presentation we do assume that  $\beta(\alpha)$  is increasing. The superinfection function  $\rho(\alpha_i - \alpha_j)$  gives the probability that, upon transmission, strain  $i$  will take over a host individual already infected with strain  $j$ . Following Pugliese (2002), we assume here that the superinfection function is increasing and differentiable everywhere, in particular at zero, with  $\rho(0) > 0$  and  $\rho'(0) \geq 0$ . We describe alternative options and the biological mechanisms underlying different choices of the superinfection function in the Discussion.

We consider three modes of host density regulation:

1. *Constant population size*: At the equilibrium population size  $\bar{N}$ , the number of births exactly balances the number of deaths (both natural and disease-induced) such that  $b = \mu + \sum_i \alpha_i I_i / \bar{N}$ . When population size is greater (smaller) than  $\bar{N}$ , then the per capita birth rate  $b$  is zero (infinity) so that  $\bar{N}$  is stable. This mode of regulation occurs if individuals occupy non-compressible territories or living sites, offspring are produced continuously at a high rate, and newborns who cannot settle into one of the  $\bar{N}$  sites die instantaneously after birth and are not counted in the effective birth rate  $b$ . With this mode of density regulation, we recover the model of Adler and Mosquera-Losada (2002). We scale density such that  $\bar{N} = 1$  without loss of generality.
2. *Constant population birth rate*:  $b(N) = B/N$  and the population-wide number of births per unit of time is constant  $B$  (this is analogous to a chemostat with constant influx). This mode of density regulation was assumed also by Boldin and Diekmann (2008). The pathogen-free host population equilibrates at  $\bar{N} = B/\mu$ ; we scale density such that  $B = \mu$  and  $\bar{N} = 1$  without loss of generality. Note that the equilibrium density of the host in the presence of the pathogen depends on the virulence and transmission rate of the pathogen, and is in general less than the pathogen-free equilibrium  $\bar{N} = 1$ .
3. *Logistic growth*:  $b(N) = r - cN$  when positive and zero otherwise, such that the host population follows logistic growth in the absence of the pathogen with equilibrium population size  $\bar{N} = (r - \mu)/c$ . With logistic growth, we recover a model of Pugliese (2002). We scale the density of hosts such that  $c = r - \mu$  and  $\bar{N} = 1$  without loss of generality. For the host to be viable,  $r$  must exceed  $\mu$ .

In all three cases, the pathogen is viable if  $\beta > \alpha + \mu$ . With a single resident pathogen strain ( $k = 1$ ), all three modes of population regulation yield a single, stable endemic equilibrium of susceptible and infected densities whenever the pathogen is viable. With two or more resident strains, however, the logistic model may yield multiple equilibria or stable population cycles (Brian Reade, cited by Pugliese, 2002).

With a single resident strain of virulence  $\alpha$ , the equilibrium density of susceptibles is

$$\hat{S}(\alpha) = \frac{\alpha + \mu}{\beta(\alpha)}, \quad (2)$$

irrespective of superinfections and the mode of host population regulation. In the absence of superinfections ( $\rho \equiv 0$ ), strains with different  $\hat{S}(\alpha)$  cannot co-exist and the evolution of

virulence minimizes  $\hat{S}(\alpha)$  and, equivalently, maximizes the basic reproduction number  $R_0(\alpha) = \beta(\alpha)/(\alpha + \mu)$  (Bremermann and Thieme, 1989; Dieckmann and Metz, 2006).

Next, we calculate the basic quantities necessary for an adaptive dynamic analysis of the model (see Geritz *et al.*, 1998). Assume that the resident population of a single strain  $\alpha$  is at its population dynamical equilibrium  $(\hat{S}(\alpha), \hat{I}(\alpha))$ . The invasion fitness of a new mutant strain with virulence  $\alpha_{\text{mut}}$  is the per capita growth rate of hosts infected with the mutant strain; from equation (1b), this is given by

$$s_a(\alpha_{\text{mut}}) = \beta(\alpha_{\text{mut}}) [\hat{S}(\alpha) + \rho(\alpha_{\text{mut}} - \alpha)\hat{I}(\alpha)] - \beta(\alpha)\rho(\alpha - \alpha_{\text{mut}})\hat{I}(\alpha) - \alpha_{\text{mut}} - \mu. \quad (3)$$

If the invasion fitness  $s_a(\alpha_{\text{mut}})$  is negative, then the mutant strain dies out; if  $s_a(\alpha_{\text{mut}})$  is positive, then the mutant has a positive probability of invasion [a selectively favoured mutant may also go extinct due to demographic stochasticity in the initial phase of invasion, when the mutant is present in only a few host individuals (cf. Jagers, 1975)].

For simplicity, we assume throughout that the environment is constant such that the resident population attains a stable fixed point  $(\hat{S}, \hat{I})$ . Note, however, that the invasion fitness is linear in  $S$  and  $I$ . This implies that in a periodic or stochastic environment, we recover the same invasion fitness as in equation (3), with  $\hat{S}$  and  $\hat{I}$  being the time average of the fluctuating population densities (Metz *et al.*, 1992).

As a result of repeated invasions and substitutions of mutations of small effect, virulence evolves in the direction of the fitness gradient,

$$D(\alpha) = \left. \frac{\partial s_a(\alpha_{\text{mut}})}{\partial \alpha_{\text{mut}}} \right|_{\alpha_{\text{mut}} = \alpha} = \beta'(\alpha) [\hat{S} + \rho(0)\hat{I}] + 2\beta(\alpha)\rho'(0)\hat{I} - 1. \quad (4)$$

At an evolutionarily singular virulence  $\alpha^*$  the fitness gradient is zero, i.e.

$$\beta'(\alpha) [\hat{S} + \rho(0)\hat{I}] + 2\beta(\alpha)\rho'(0)\hat{I} = 1 \quad (5a)$$

is satisfied at  $\alpha = \alpha^*$ . Using the basic reproduction number,  $R_0(\alpha) = \beta(\alpha)/(\alpha + \mu)$ , this equation can be rewritten as

$$R_0'(\alpha) \frac{(\alpha + \mu)^2}{\beta(\alpha)} + \hat{I}[\beta'(\alpha)\rho(0) + 2\beta(\alpha)\rho'(0)] = 0, \quad (5b)$$

and since the second term in the left-hand side is positive, we find that singular strategies can only be found in the region where  $R_0'(\alpha) < 0$  [compare with Proposition 3 of Pugliese (2002)]. Superinfections drive the evolution of virulence beyond the point that maximizes  $R_0$  for two reasons. First, when  $\rho(0) > 0$ , superinfection events shorten the average lifetime of an infection and therefore select for high transmission and high virulence. This is analogous to the effect of the natural death rate in the absence of superinfections: for high values of  $\mu$ , a high level of virulence maximizes  $R_0$  (Van Baalen and Sabelis, 1995). Second,  $\rho'(0) > 0$  means that virulence *higher* than that of the resident strains provides competitive advantage in superinfections. This drives an evolutionary arms race in virulence analogous to arms races in size, weaponry, and other traits conferring advantage in asymmetric competition (Parker, 1983; Maynard Smith and Brown, 1986; Matsuda and Abrams, 1994).

The singular strain  $\alpha^*$  is evolutionarily stable if the second derivative

$$E = \left. \frac{\partial^2 s_a(\alpha_{\text{mut}})}{\partial \alpha_{\text{mut}}^2} \right|_{\alpha_{\text{mut}} = \alpha} = \beta''(\alpha) [\hat{S} + \rho(0)\hat{I}] + 2\beta'(\alpha)\rho'(0)\hat{I} \quad (6a)$$

is negative at  $\alpha = \alpha^*$ , and it *lacks* evolutionary stability if

$$\beta''(\alpha) > -\frac{2\beta'(\alpha)\rho'(0)\hat{I}}{\hat{S} + \rho(0)\hat{I}}. \quad (6b)$$

Note that with  $\beta'(\alpha) > 0$  and  $\rho'(0) > 0$ , the singular point lacks evolutionary stability also with some concave trade-offs.

There are pairs of strains in the neighbourhood of the singular point that can mutually invade each other's population and hence co-exist if the cross-derivative

$$M = \frac{\partial^2 s_a(\alpha_{\text{mut}})}{\partial \alpha_{\text{mut}} \partial \alpha} \Big|_{\alpha_{\text{mut}} = \alpha} = \beta'(\alpha) \frac{d[\hat{S} + \rho(0)\hat{I}]}{d\alpha} + 2\beta(\alpha)\rho'(0) \frac{d\hat{I}}{d\alpha} \quad (7)$$

is negative at  $\alpha = \alpha^*$ . If  $M$  is positive, then there are pairs with mutual exclusion, i.e. such that neither can spread in the population of the other.

### CRITICAL FUNCTION ANALYSIS

The value and stability properties of  $\alpha^*$  can only be determined if one specifies the trade-off function between transmission and virulence,  $\beta(\alpha)$ . With critical function analysis, we turn the question around and ask which properties the trade-off function should exhibit if a strain with given virulence and transmission ( $\alpha$ ,  $\beta$ ) is to be a convergence stable ESS, an evolutionary branching point or a repeller. Below we give a short summary of the method; see de Mazancourt and Dieckmann (2004) and Kisdi (2006) for a full account. Svennungsen and Kisdi (*in press*) explain critical function analysis specifically in the context of virulence evolution in a single-infection model, and the examples in the next section illustrate the predictions of the critical function analysis.

A strain ( $\alpha$ ,  $\beta$ ) is singular if equation (5a) is satisfied, i.e. if

$$\beta'(\alpha) = \frac{1 - 2\beta(\alpha)\rho'(0)\hat{I}}{\hat{S} + \rho(0)\hat{I}} \quad (8)$$

holds at ( $\alpha$ ,  $\beta$ ); recall that  $\hat{S}$  and  $\hat{I}$  depend on the chosen value of  $\alpha$  and  $\beta$  via equations (1),  $k = 1$ . The critical functions  $\beta_{\text{crit}}(\alpha)$  are the solutions of the ordinary differential equation in equation (8) (with different initial values) and depend on the form of host density regulation (choice of  $b(N)$ ) as well as on model parameters  $\rho(0)$ ,  $\rho'(0)$ , and  $\mu$ . Geometrically, the slope of the critical functions show at every point of the  $\alpha$ ,  $\beta$  plane which slope the trade-off function needs to have if ( $\alpha$ ,  $\beta$ ) is to be singular; at the singular point, the trade-off is tangential to a critical function. Furthermore, the singular point is convergence stable (attracting) if the trade-off is locally more concave (or less convex) than the critical function (de Mazancourt and Dieckmann, 2004).

To determine if evolutionary branching is possible at a point ( $\alpha$ ,  $\beta$ ) if the trade-off is chosen such that this point is singular, we calculate the cross-derivative  $M$ , defined in (7), at this point.  $M$  depends on the slope, but not on the convexity, of the trade-off function. Since the slope is fixed by the singularity condition in equation (8), each point of the  $\alpha$ ,  $\beta$  plane can be characterized with a positive or negative value of  $M$ . If ( $\alpha$ ,  $\beta$ ) is to be an evolutionary branching point, then it must be convergence stable and hence the trade-off must be chosen more concave than the critical function; and at the same time ( $\alpha$ ,  $\beta$ ) must not be evolutionarily stable, hence the trade-off must be chosen convex enough to satisfy

inequality (6b) [note that every quantity on the right-hand side of (6b) is fixed by the choice of  $(\alpha, \beta)$  and the singularity condition]. Using the results of Bowers *et al.* (2005), Kisdi (2006) showed that this choice is possible if and only if  $M$  is negative at point  $(\alpha, \beta)$ . If  $M$  is positive at every point of the  $\alpha, \beta$  plane, then evolutionary branching is not possible under any trade-off (see such a case below).

Convergence stable ESSs can easily be obtained by choosing a trade-off function that is tangential to a critical function at  $(\alpha, \beta)$  and which is sufficiently concave at this point to ensure that it is more concave than the critical function as well as concave enough for  $E$  in (6a) to be negative. If the trade-off is tangential to a critical function but less concave than the critical function itself, the resulting singular point is a repeller. Note that although the existence of an evolutionary branching point depends on the sign of  $M$ , a convergence stable ESS or a repeller can be obtained at any point by choosing an appropriate trade-off function.

In the absence of superinfections ( $\rho(0) = 0, \rho'(0) = 0$ ), equation (8) simplifies to  $\beta'(\alpha) = 1/\hat{S} = \beta(\alpha)/(\alpha + \mu)$ , the solutions of which are straight lines,  $\beta_{\text{crit}}(\alpha) = \beta_{\text{crit}}(0)(\alpha + \mu)/\mu$ . A singularity is therefore convergence stable if and only if the trade-off is locally concave. According to (6a), this is precisely the condition for evolutionary stability ( $E < 0$ ) as well. Without superinfections, all ESSs are thus convergence stable and all singularities that are not ESSs are repellers. The expression in (7) simplifies to  $M = \beta'(\alpha)d\hat{S}/d\alpha$ ; by substituting  $\hat{S}$  from equation (2) and the slope  $\beta'(\alpha)$  with the slope of the critical function,  $M$  turns out to be zero, i.e. neither mutual invasibility nor mutual exclusion occurs. These local results are due to the fact that without superinfections, evolution optimizes  $R_0$  (Bremermann and Thieme, 1989).

It is also easy to see that the border of pathogen viability is always a critical function. When  $\hat{I} = 0$ , equation (8) again simplifies to  $\beta'(\alpha) = 1/\hat{S} = \beta(\alpha)/(\alpha + \mu)$ , which is satisfied by the function  $\beta(\alpha) = (\alpha + \mu)/\bar{N}$ , the border of viability. By continuity, critical functions in the vicinity of the border of viability are also nearly linear. In this region  $\hat{I}$  is small, hence  $E$  changes sign when the trade-off is nearly linear. Close to the border of viability, therefore, the model behaves almost as an optimization model, and even if  $M$  is negative, evolutionary branching occurs in only a narrow range of parameters (this range shrinks to zero as the border of viability is approached).

Next, we present the results of critical function analysis for the three different modes of host density regulation introduced above. In all figures, we scale time such that the expected lifetime of an uninfected host ( $1/\mu$ ) is the unit of time, i.e.  $\mu = 1$  and all quantities are dimensionless (host population density has been scaled such that  $\bar{N} = 1$  in each of the three models). Note that scaling time affects the numerical values of  $\alpha$  and  $\rho'(0)$ : If the infection dynamics are (considerably) faster than other demographic processes of the host, then  $\alpha$  assumes values (considerably) greater than 1, and the numerical value of  $\rho'(0)$  is small.  $\beta$  assumes large values both because the unit of density is large ( $\bar{N} = 1$ ) and because the time unit is long compared with the infection dynamics.

### Constant population size

Calculations are relatively easy if total population size is constant ( $\hat{N} \equiv 1$ ), and therefore the population dynamic equilibrium of equations (1) for  $k = 1$  is simply  $\hat{S} = (\alpha + \mu)/\beta(\alpha)$  and  $\hat{I} = 1 - (\alpha + \mu)/\beta(\alpha)$ . A straightforward, exact calculation [using equation (8) for the slope  $\beta'(\alpha)$  in (7)] shows that within the region of viability,  $M$  is negative when  $\beta > \beta_M = (1 - \rho(0))/2\rho'(0)$  and positive otherwise.

If  $\rho(0)$  is set to be zero, then equation (8) can be solved analytically to obtain

$$\beta_{\text{crit}}(\alpha) = \frac{\beta_{\text{crit}}(0)(\alpha + \mu)}{\beta_{\text{crit}}(0) - (\beta_{\text{crit}}(0) - \mu)e^{-2\rho'(0)\alpha}}, \quad (9)$$

where  $\beta_{\text{crit}}(0)$  is the initial value that varies among critical functions. Our model assumes  $\rho(0) > 0$ , but realistic values of  $\rho(0)$  are close to zero (see Discussion). The critical functions in Fig. 1, obtained by numerical solution of equation (8) with  $\rho(0) = 0.01$ , are close to the

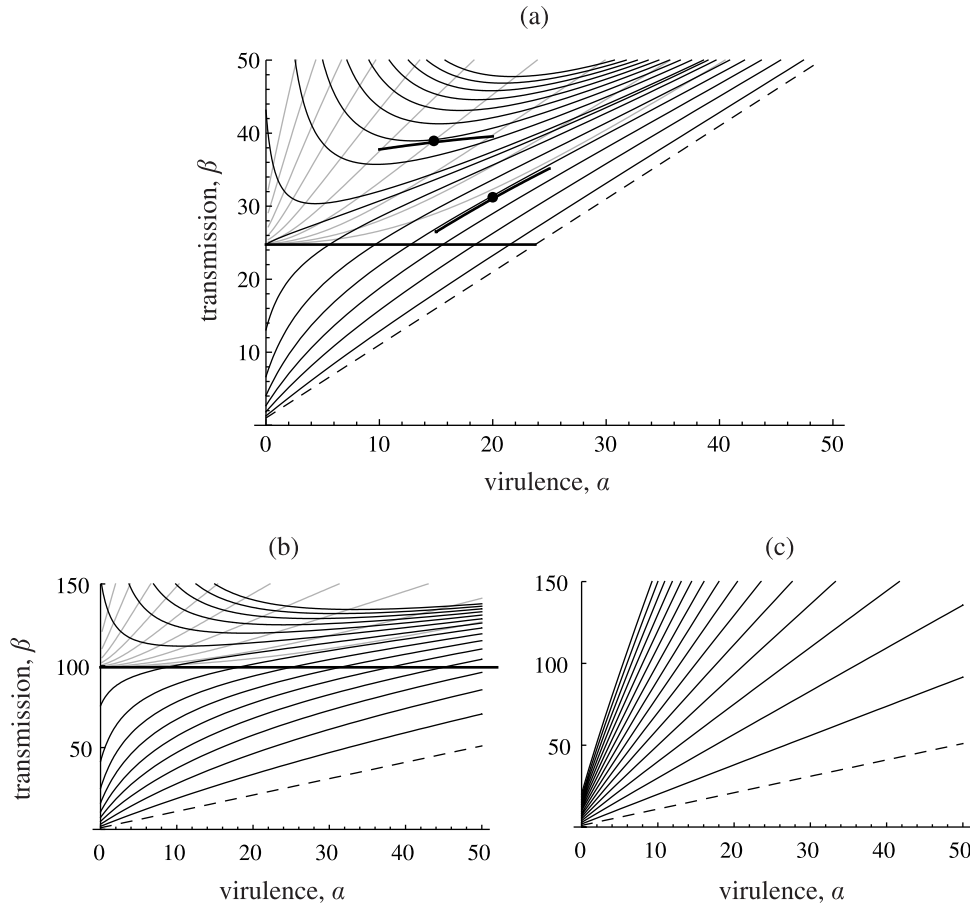


**Fig. 1.** Constant population size. Critical functions are shown as thin black lines; the lowermost critical function coincides with the border of pathogen viability (dashed).  $M$  is negative above the thick horizontal line at  $\beta_M$  and positive below (in (c),  $M$  is positive whenever the pathogen is viable). The thin grey lines are contour lines of the convexity range permitting evolutionary branching, with contours drawn at values (0.01, 0.02, 0.04, 0.08, 0.16, 0.32, 0.64, 1.28, 2.56, 5.12) [when less than 10 contour lines are shown, the first values of the list apply]. In (a), segments of the most concave trade-off leading to evolutionary branching at the highlighted point are shown at two points (note that the convexity of the trade-off matters only locally; relatively long segments are shown for visual clarity). Parameter values are  $\mu = 1$ ,  $\rho(0) = 0.01$ , and (a)  $\rho'(0) = 0.02$ , (b)  $\rho'(0) = 0.005$ , (c)  $\rho'(0) = 0$ . Note the different vertical scales.

curves given by equation (9) (the fit is best in Fig. 1a and becomes worse for smaller values of  $\rho'(0)$ ).

In Fig. 1a, the critical functions are concave at low transmission rates such that only concave trade-offs can result in a convergence stable singularity. Evolutionary branching is not possible for  $\beta < \beta_M$  (below the thick line) because  $M$  is positive. At higher transmission rates and low values of virulence, the critical functions are decreasing: The advantage of increasing virulence via enabling superinfections is so great that it could balance some loss in the transmission rate. Since we assume that the trade-off is an increasing function (i.e. higher virulence implies higher transmission), the trade-off cannot tangent a critical function in this region and hence no singularities occur. (It is conceivable that hosts infected by more virulent strains become increasingly immobilized so that they do not encounter other hosts, and this could result in decreasing trade-off functions.) Evolutionary branching is possible above the  $\beta = \beta_M$  line and at sufficiently high virulence such that the critical function is increasing.

To see how likely evolutionary branching is, we compute the range of convexity the trade-off can assume to obtain branching (cf. de Mazancourt and Dieckmann, 2004), i.e. the difference between the maximum value of  $\beta''(\alpha)$  set by the convexity of the critical function and the minimum value of  $\beta''(\alpha)$  set by inequality (6b), at every point  $(\alpha, \beta)$  where  $M$  is negative. The results are shown with grey contour lines in Fig. 1a. Evolutionary branching is thus most likely if the singularity is at low virulence and high transmission (but assuming increasing trade-offs, the singularity needs to be right of the minimum of the critical function). At two points in Fig. 1a, we show segments of the most concave trade-off that still leads to evolutionary branching: a trade-off lying locally between the critical function and the segment will lead to evolutionary branching at the point highlighted.

As  $\rho'(0)$  decreases, the minimum transmission for evolutionary branching,  $\beta_M$ , increases (Fig. 1b). This progressively limits the possibility of branching. When both  $\rho'(0)$  and  $\rho(0)$  are close to zero, the critical functions are nearly linear (Fig. 1c) and the model is close to an optimization model (see above).

It is noteworthy that for  $\beta < \beta_M$ ,  $M$  is positive. Superinfection is generally regarded as a mechanism that promotes co-existence by mutual invasibility; a positive value of  $M$  however implies the opposite, i.e. mutual exclusion between pairs of strains, such that neither strain can spread in the established population of the other (Geritz *et al.*, 1998).

Suppose now that the probability of superinfection is independent of virulence ( $\rho'(0) = 0$ ), whereas  $\rho(0) > 0$  is arbitrary. This situation occurs if the success of the superinfection is determined either by random factors or pathogen traits not related to its virulence. In this case, equation (8) can be solved analytically for the inverse critical functions,

$$\alpha = (\beta_{\text{crit}}(\alpha) - \mu) - (\beta_{\text{crit}}(0) - \mu) \left( \frac{\beta_{\text{crit}}(\alpha)}{\beta_{\text{crit}}(0)} \right)^{1 - \rho(0)}. \quad (10)$$

Since the inverse functions are convex, the critical functions are always concave such that the trade-off also needs to be concave to have a convergence stable singular point (although the critical functions are close to linear when  $\rho(0)$  is close to zero, as in Fig. 1c). Moreover,  $M$  is positive everywhere [as  $\rho'(0)$  goes to zero,  $\beta_M = (1 - \rho(0))/2\rho'(0)$  goes to infinity], and evolutionary branching is not possible. Therefore,  $\rho'(0) > 0$  is essential for evolutionary branching in this model (but not under other modes of host density regulation; see below).

### Constant population birth rate

With constant population birth rate, the population dynamic equilibrium of equations (1) (with  $k = 1$ ) is  $\hat{S} = (\alpha + \mu) / \beta(\alpha)$  and  $\hat{I} = \mu / (\alpha + \mu) - \mu / \beta(\alpha)$ . Substituting this equilibrium into the fitness function,  $M$  can be obtained as

$$M = - \frac{\beta \mu^2 (\beta - \alpha - \mu) [\rho(0) + 2(\alpha + \mu) \rho'(0)]^2}{(\alpha + \mu) [(\alpha + \mu)^2 + \mu(\beta - \alpha - \mu) \rho(0)]^2}. \quad (11)$$

Because  $\beta > \alpha + \mu$  whenever the pathogen is viable,  $M$  is always negative if  $\rho(0)$  or  $\rho'(0)$  is greater than zero (when both are zero, superinfections are absent and the model reduces to an optimization model; see above). Superinfections thus facilitate co-existence even if higher virulence gives no advantage in superinfection ( $\rho'(0) = 0$ ; note that the opposite result was found for the case of constant population size). As before, equation (8) can be solved analytically for the critical functions in the limiting case  $\rho(0) = 0$ :

$$\beta_{\text{crit}}(\alpha) = \frac{\beta_{\text{crit}}(0)(\alpha + \mu)}{\beta_{\text{crit}}(0) - (\beta_{\text{crit}}(0) - \mu) [\mu / (\alpha + \mu)]^{2\rho'(0)\mu}}, \quad (12)$$

and the numerical solutions of equation (8) shown in Fig. 2 are qualitatively similar to the curves specified by equation (12).

Of the three modes of density regulation considered, the case of constant population birth rate is the most conducive to evolutionary branching:  $M$  is always negative whenever the pathogen is viable, permitting branching everywhere if the trade-off is chosen appropriately. The trade-off can be chosen from a relatively broad range of convexity also in the part where the critical functions are increasing, i.e. where a singular strategy is possible with an increasing trade-off (Fig. 2a).

Recall that critical functions are decreasing where the competitive advantage of higher virulence during superinfections is so high that it can compensate even for a decrease in the transmission rate. For greater values of  $\rho'(0)$  this happens in a larger area of the  $(\alpha, \beta)$  plane, i.e. the minima of the critical functions shift towards the right. Conversely, as  $\rho'(0)$  decreases, the minima of the critical functions move to the left and disappear (Fig. 2b, c). Evolutionary branching remains possible also with arbitrarily small  $\rho'(0)$ , but the most likely branching points shift towards low virulence.

### Logistic growth

When the host population obeys logistic growth in the absence of the pathogen, the equilibrium density of the infected hosts is given by a more lengthy formula and we could obtain results only numerically. In Fig. 3a, the critical functions are qualitatively similar to the case of constant population birth rate (compare with Fig. 2a), but  $M$  is positive and thus evolutionary branching is excluded for low transmission rates (below the thick line). As  $\rho'(0)$  decreases (Fig. 3b, c), evolutionary branching remains possible but the area of positive  $M$  increases, limiting the possibility for branching and indicating that mutual exclusion rather than co-existence becomes more common. In the previous cases, we found that analytic solutions with  $\rho(0) = 0$  were similar to the critical functions obtained numerically for  $\rho(0) = 0.01$  (recall that realistic values of  $\rho(0)$  are small). In the logistic case, equation (8) cannot be solved analytically but decreasing the value of  $\rho(0)$  does not change the curves appreciably (Fig. 3d).

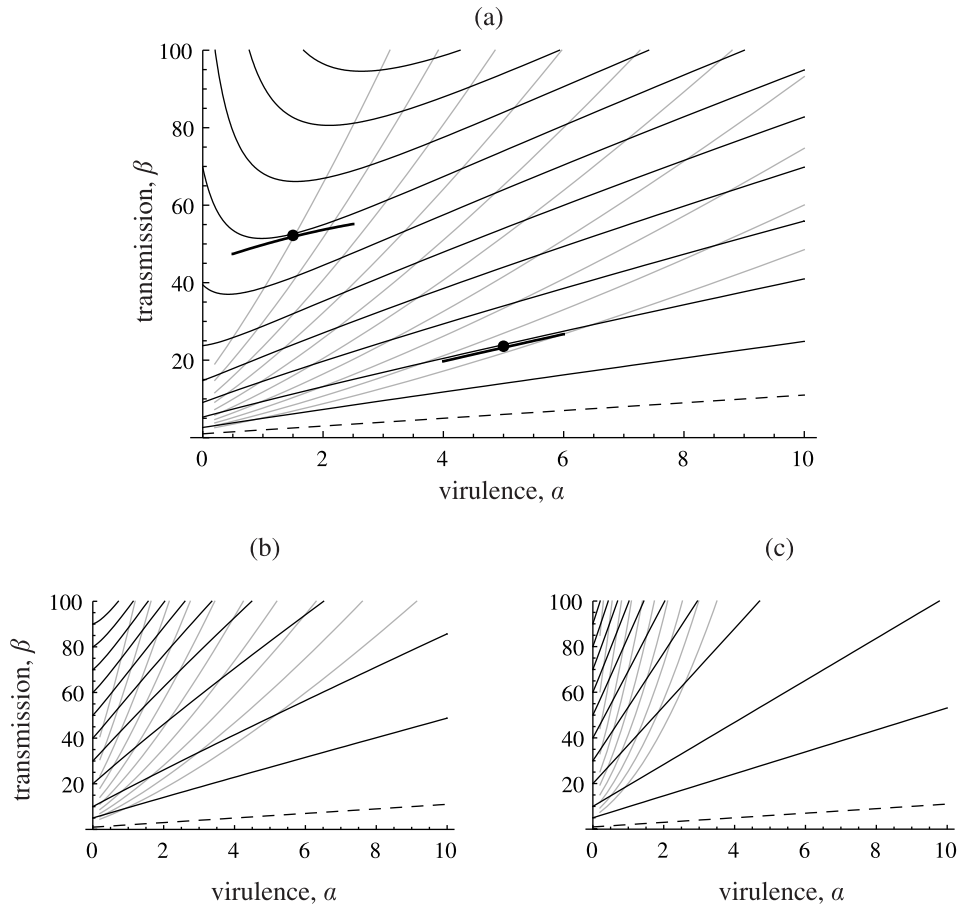


**Fig. 2.** Constant population birth rate. Notations and parameter values are as in Fig. 1, with the exception that  $M$  is negative at every point where the pathogen is viable.

The logistic model has one more parameter, the maximum per capita birth rate ( $r$ ). Since we scale the pathogen-free population density to 1 by setting  $c = r - \mu$  in the logistic equation,  $r$  parameterizes the strength of density regulation: when  $r$  takes a high value, the population returns to its equilibrium quickly. With the pathogen present but with  $r \gg \alpha, \beta$ , the infection has only a negligible effect on total population size. This implies that as  $r$  increases, the critical functions converge to the case of constant population size (see Fig. 1).

The host population is viable only if  $r > \mu$ . When  $r$  decreases towards  $\mu$ , the likely points of evolutionary branching shift towards lower virulences (Fig. 3e); comparing the same point ( $a, \beta$ ) across different values of  $r$  (e.g. in Fig. 3a and 3e), evolutionary branching becomes less likely as  $r$  decreases. To explain this change, recall from equations (1) that with a single pathogen ( $k=1$ ), total population density  $N = S + I$  grows according to  $dN/dt = N[b(N) - \mu - (I/N)\alpha]$ . Since  $b(N) < r$ ,  $(I/N)\alpha$  cannot exceed  $r - \mu$  in equilibrium. If  $r$  decreases towards  $\mu$  (while we keep  $a$  and  $\beta$  fixed),  $(\hat{I}/\hat{N})$  must decrease to zero and thus in the limit the density of infected vanishes [whereas  $\hat{S} = (\alpha + \mu)/\beta$  is fixed and  $\hat{N}$  goes to  $\hat{S}$ ]. This implies that superinfections disappear, and, as discussed above, the model becomes an

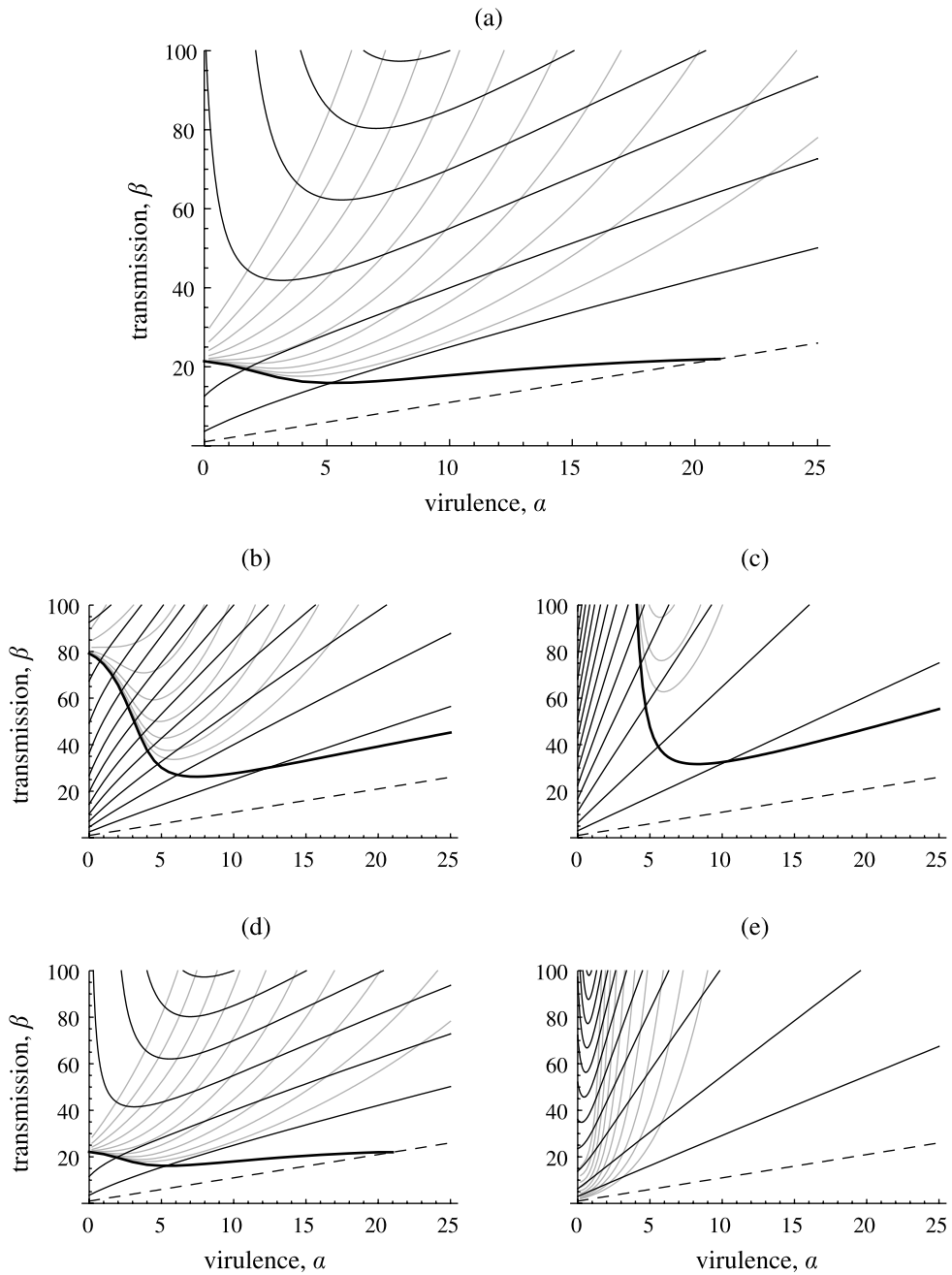


**Fig. 3.** Logistic population growth. Notations as in Fig. 1.  $M$  is negative above the thick curve and positive below it; in (e),  $M$  is negative whenever the pathogen is viable. In panel (a), parameter values are  $\mu = 1$ ,  $r = 10$ ,  $\rho(0) = 0.01$ , and  $\rho'(0) = 0.02$ ; in panels (b–e), parameters are as in (a) except (b)  $\rho'(0) = 0.005$ , (c)  $\rho'(0) = 0$ , (d)  $\rho(0) = 0.001$ , and (e)  $r = 2$ .

optimization model. In particular, in the limit  $r \rightarrow \mu$  and hence  $\hat{I} \rightarrow 0$ , the critical functions from equation (8) become straight lines such that a singular point is convergence stable if and only if the trade-off is concave. The condition for evolutionary stability (i.e.  $E$  in (6a) is negative) reduces to  $\beta''(\alpha) < 0$  such that every convergence stable singularity is an ESS, leaving no possibility for evolutionary branching. The speed of convergence depends on the virulence: with a high value of  $\alpha$ ,  $\hat{I}/\hat{N}$  must be smaller to make  $(I/N)\alpha$  less than  $r - \mu$ . In Fig. 3e, the limit is not reached yet, but conditions for branching are very restrictive except at low values of virulence. Note that similar results should hold for any mode of density regulation where the per capita birth rate is bounded; with the assumption of constant population size or constant population birth rate, however, this is not the case.

### ADAPTIVE DYNAMICS AND BIFURCATION ANALYSIS: EXAMPLES

In this section, we illustrate the results of the critical function analysis with examples from the constant population birth rate model, using standard techniques of adaptive dynamics (see Geritz *et al.*, 1998).

#### Adaptive dynamics in selected examples of virulence evolution

In Figs. 4 and 5, we show examples of adaptive dynamics in monomorphic and dimorphic pathogen populations. For modelling the co-evolution of two strains, we need to specify the superinfection function; hence we choose

$$\rho(\alpha_2 - \alpha_1) = \frac{A}{A + (1 - A)e^{-B(\alpha_2 - \alpha_1)}}, \quad (13)$$

where the constants  $A$  and  $B$  relate to the value and slope of the superinfection function at zero according to  $A = \rho(0)$  and  $B = \rho'(0)/[\rho(0)(1 - \rho(0))]$ .

An example of evolutionary branching is shown in Fig. 4, where we used a concave, fast saturating trade-off (Fig. 4b). When  $\rho'(0)$  is small enough such that the critical functions become increasing before the trade-off saturates, a quickly saturating trade-off typically tangents a critical function in or near the region where saturation occurs. Note that the second derivative of the trade-off,  $\beta''(\alpha)$ , changes rapidly in this region. In Fig. 4, the trade-off is nearly linear at the point of tangent to a critical function, such that condition (6b) is satisfied and the singularity is an evolutionary branching point (this may be hard to judge from the pairwise invasibility plot shown in Fig. 4a, but is confirmed by the enlarged plot showing the fitness gradients in the vicinity of the singularity in Fig. 4e). With small changes in parameter values, however, the point of tangent in Fig. 4b may shift to the strongly concave part of the trade-off, resulting in an ESS rather than a branching point.

Following evolutionary branching, the two co-existing strains undergo parallel evolution towards higher virulence: an evolutionary arms race occurs. Note that the direction of evolution changes after evolutionary branching: in monomorphic populations virulence evolves downwards over the same range where dimorphic populations exhibit an arms race towards high levels of virulence (Fig. 4d). The area of co-existence attached to the branching point forms a narrow corridor (Fig. 4c), but the boundaries of the corridor are repelling such that the evolutionary dynamics keep the population within the narrow area where two strains co-exist. The evolutionary arms race ends at the upper end of the corridor, where the

two strains attain a dimorphic evolutionary singularity at the intersection of isoclines (Fig. 4f). At this point, the less virulent strain undergoes evolutionary branching, yielding three co-existing pathogen strains (not shown).

Pugliese (2002) proved for a class of concave trade-offs that every monomorphic singularity is an ESS. In Fig. 5, we show the adaptive dynamics of virulence with the hyperbolic trade-off  $\beta(a) = 30a/(1 + a)$ , which is an example from Pugliese's class. The critical functions (Fig. 5b) indicate that evolutionary branching would be possible if the trade-off were chosen to be less concave at the singular point; this is however not possible within the family of hyperbolic trade-offs of the form  $\beta(a) = ka/(c + a)$ . Nevertheless, the singularity is close to the bifurcation point between an ESS and a branching point.

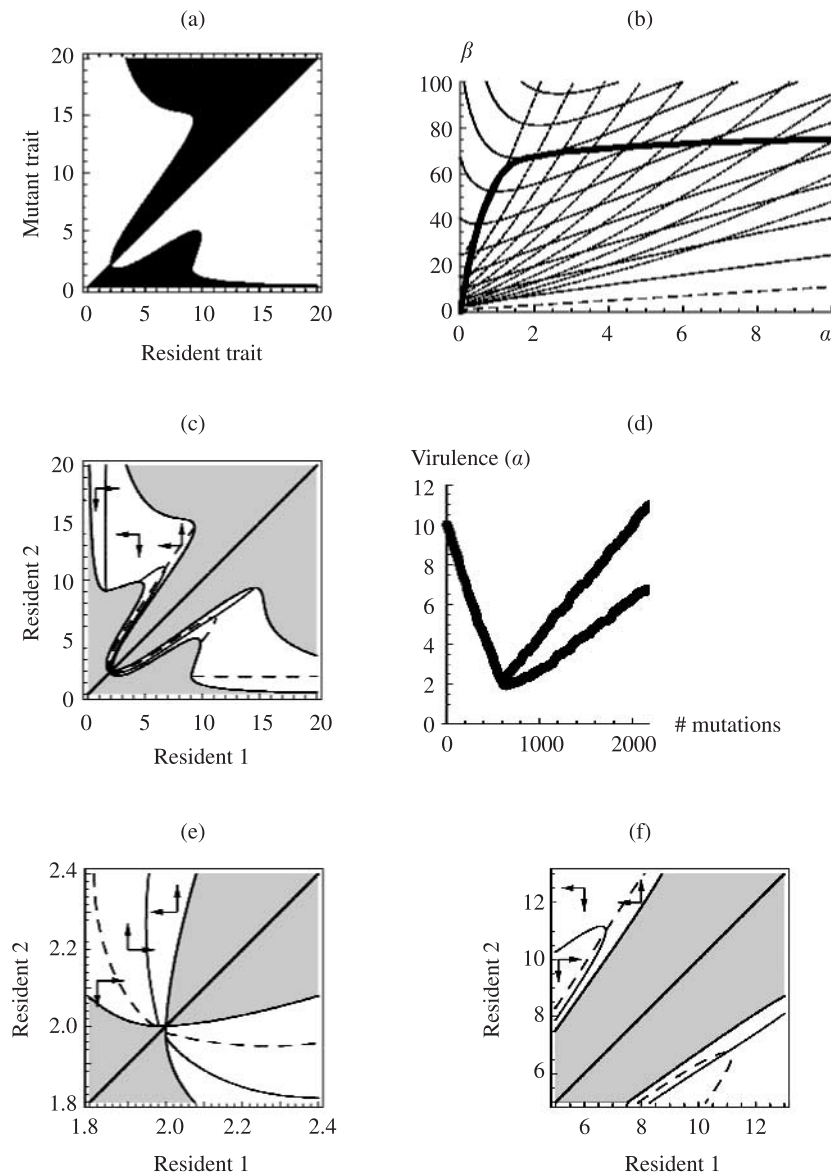


Figure 5e shows the fitness gradients of dimorphic populations in a neighbourhood of the monomorphic singularity. Near the ESS, co-existing strains always converge towards one another and towards the ESS. When a monomorphic population evolves towards the ESS, it may temporarily become dimorphic in the vicinity of the singularity, but every dimorphism is eventually resolved at the ESS (cf. Fig. 5d). This prediction, however, holds only if mutation steps do not exceed a maximum size, and the maximum gets smaller when the model is approaching a bifurcation point. Because the ESS in Fig. 5 is close to bifurcating into a branching point, areas of different dimorphic fitness gradients exist relatively close to the ESS (shown by arrows and separated by the isoclines in Fig. 5e). With sufficiently large mutations, it is possible to step into the area of co-existence above the dashed isocline in Fig. 5e. Here the strains are subject to parallel selection (between the isoclines) or disruptive selection (above the continuous isocline), and can therefore diverge from one another (Fig. 5f). Note that at the point of bifurcation itself, the same happens with arbitrarily small mutations.

### Bifurcation analysis of adaptive dynamics

Next we show how a classic bifurcation analysis of monomorphic evolutionary singularities relates to the critical function analysis presented earlier. Since here we deal only with monomorphic singularities, it suffices to specify the values of  $\rho(0)$  and  $\rho'(0)$ ; the shape of the superinfection function away from zero is irrelevant. For the trade-off function, we choose the three-parameter family

$$\beta(\alpha) = a + b\alpha - ae^{-c\alpha} \quad (14)$$

---

**Fig. 4.** Evolutionary branching and co-evolution of co-existing strains assuming constant population birth rate, the superinfection function given in equation (13) with  $\rho(0) = 0.02$  and  $\rho'(0) = 0.02$ , the trade-off function shown in panel (b) (obtained as an Interpolation function in *Mathematica* with the following points and derivatives:  $(\alpha, \beta) = (0,0)$ ;  $(2, 67.5889)$  with slope 2.73486 [tangent to a critical function] and second derivative  $-0.1$ ;  $(3, 70)$  with slope 1.4;  $(10, 75)$  with slope 0.2;  $(20, 76)$  with slope 0), and  $\mu = 1$ . (a) Pairwise invasibility plot. The mutant's invasion fitness is positive in the white areas (invasion) and negative in the black areas (no invasion). There is an evolutionary branching point at  $\alpha^* = 2.0$ . The resident strain is viable for  $0.0106 < \alpha < 59.4427$ . (b) The trade-off function superimposed on the critical functions (notations as in Fig. 2). (c) Area of co-existence and dimorphic evolution. Two resident strains can co-exist in the white area. The arrows show the direction of evolution. The first resident's fitness gradient changes sign across the continuous isoclines (zero fitness gradient horizontally); the second resident's isoclines are shown by dashed lines (zero fitness gradient vertically). The fitness gradient vanishes in both strains at the dimorphic singularity (intersection of isoclines). (d) Simulated evolutionary tree. Each step on the horizontal axis corresponds to the invasion attempt of one randomly generated mutant (maximum mutation size 0.05). The vertical axis shows the virulence of the resident strain(s) when the population has equilibrated after invasion. (e) Enlargement of (c) near the monomorphic singularity. In the immediate vicinity of the singular strategy, the two co-existing strains evolve away from one another, i.e. evolutionary branching occurs. (f) Enlargement of (c) near the dimorphic singularity. The singular dimorphism (at the intersection of isoclines) is absolutely convergent stable (Matessi and Di Pasquale, 1996) but not evolutionarily stable for the strain with lower virulence, which will undergo further evolutionary branching.

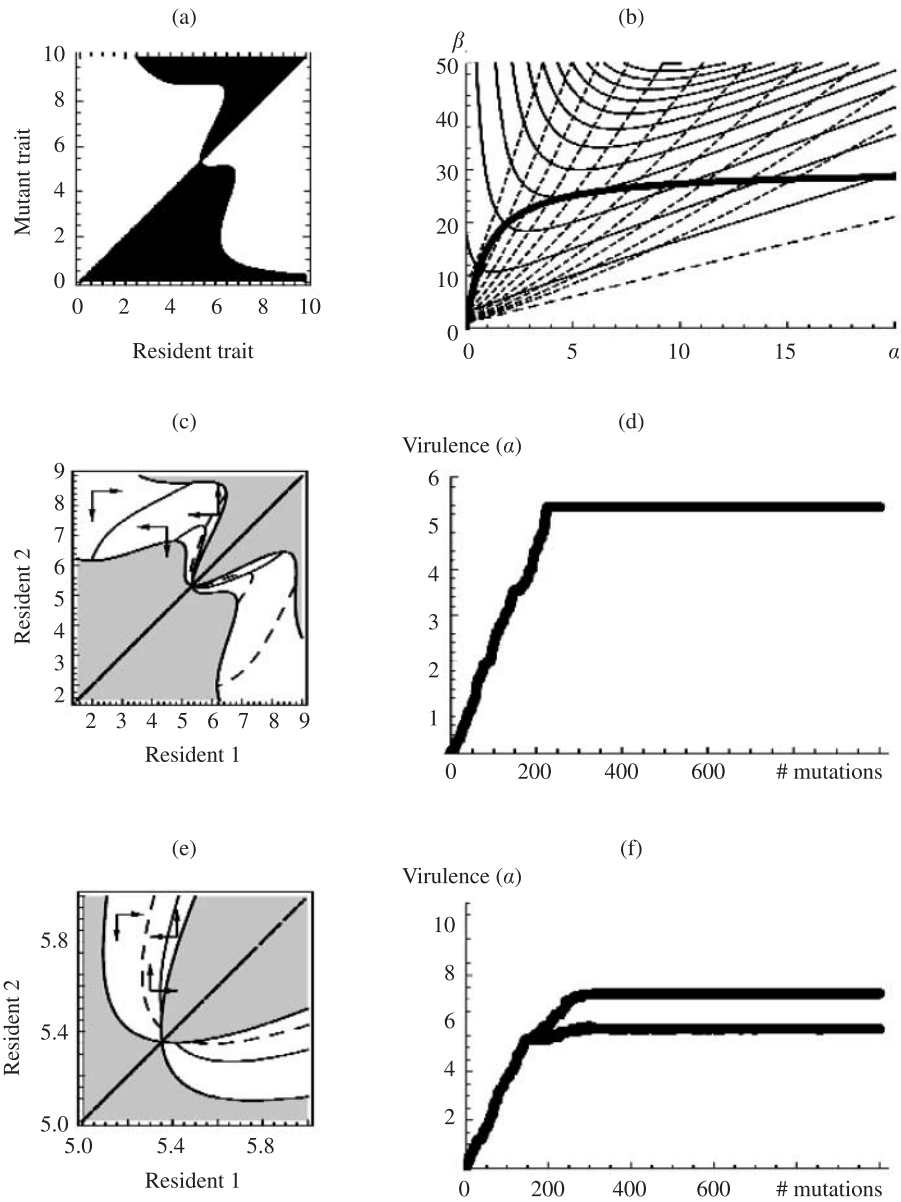
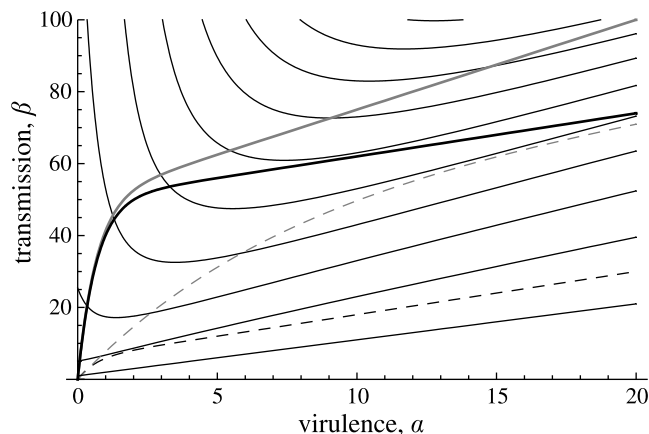


**Fig. 5.** Evolutionary dynamics with a single ESS in the model with constant population birth rate, assuming the superinfection function of equation (13) with  $\rho(0) = 0.1$  and  $\rho'(0) = 0.135$ , the trade-off function  $\beta(a) = 30a/(1 + a)$ , and  $\mu = 1$ . Notations as in Fig. 4. (a) Pairwise invasibility plot. The resident population is viable for  $0.03576 < a < 27.9642$ ; the ESS is at  $a^* = 5.35225$ . (b) The trade-off function superimposed on the critical functions. (c) Area of co-existence and dimorphic evolution. (d) Simulated evolutionary tree with maximum mutation size of 0.1. (e) Enlargement of (c) in the neighbourhood of the ESS. Note that in the immediate neighbourhood of the monomorphic singularity, the two co-existing strains evolve towards each other (stabilizing selection), and hence any dimorphism will be resolved at the ESS. With somewhat larger mutations, however, a single evolutionary step may bring the population above the dashed isocline, from which part the two strains can evolve apart. (f) Simulated evolutionary tree with maximum mutation size of 0.15.

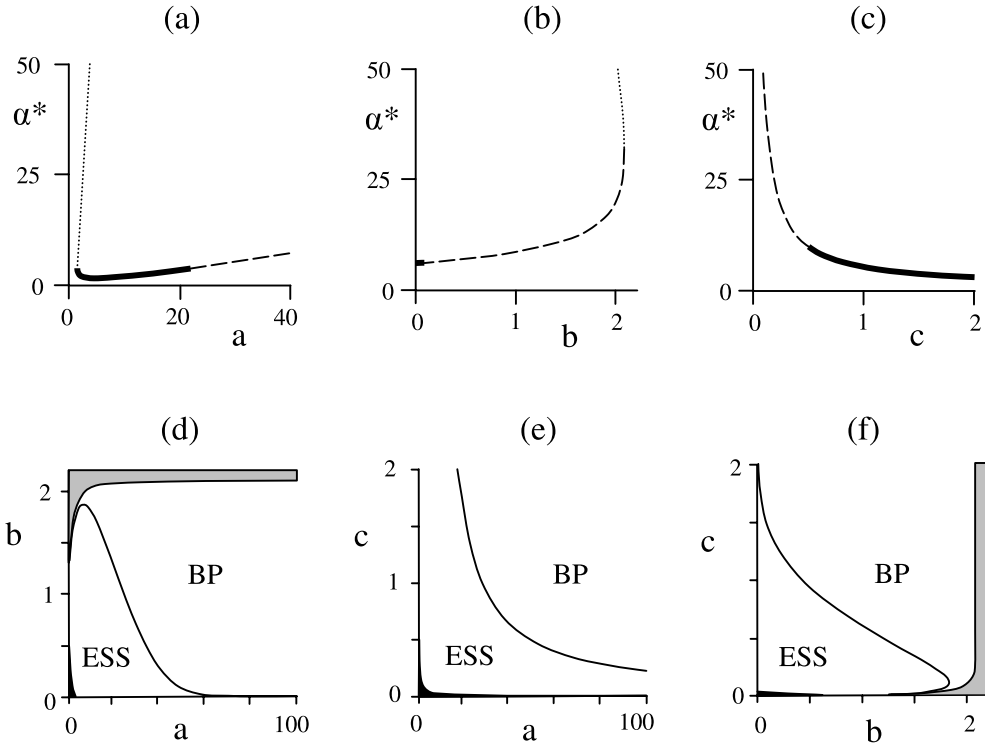
and investigate the bifurcations of monomorphic evolutionary singularities when parameters  $a$ ,  $b$ , and  $c$  are varied. The trade-off function in (14) is exponentially convergent to a straight line with slope  $b$  and intercept  $a$ . It is probably unrealistic to assume that the transmission rate can increase indefinitely, but the trade-off may well have an approximately linear segment. We thus think of the trade-off in (14) as part of a function that eventually saturates, but saturation occurs outside the range of virulence considered here.

Figure 6 shows the shape of the trade-off for a few sets of parameter values  $(a, b, c)$ , overlaid the critical functions derived in the previous section. Comparison with the critical functions immediately suggests some bifurcation patterns, which are confirmed by the formal bifurcation analysis below; we summarize these patterns as valid for most of the parameter space and refer to the exact bifurcation plots in Fig. 7 for the complete picture. As  $a$  increases, the point of tangent between the trade-off and a critical function shifts to the right, i.e. the monomorphic singularity is at a higher virulence (compare the black continuous and black dashed trade-offs in Fig. 6). At the same time, the point of tangent shifts from the strongly concave to the approximately linear part of the trade-off. With convex critical functions, this does not affect convergence stability but signals a bifurcation from an ESS to a branching point (recall from equation (6) that the singularity is an ESS if the trade-off is sufficiently concave, but it lacks evolutionary stability if the trade-off increases linearly). Increasing  $b$  also shifts the singularity towards higher virulence; when  $b$  exceeds the limiting slope of the critical functions, no singularity occurs and virulence evolves to ever higher values (i.e. until the trade-off eventually saturates outside the range shown in Fig. 6). When  $c$  is small such that the trade-off converges only slowly to a straight line, the singularity falls in the concave part of the trade-off and may be an ESS. In contrast, with large values of  $c$ , the trade-off quickly converges to the line  $a + ba$ . Given that the critical functions are convex, the singularity is then a branching point and its position is independent of  $c$ .

These expectations are confirmed by the one- and two-parameter bifurcation diagrams in Fig. 7. To obtain these bifurcation plots, we used equations (1) and (5a) with the trade-off



**Fig. 6.** Trade-off functions of the family in (14), shown together with the critical functions. Parameters are  $(a, b, c) = (50, 1.2, 1.5)$  for the black continuous trade-off;  $(50, 2.5, 1.5)$  for the grey continuous trade-off;  $(6, 1.2, 1.5)$  for the black dashed trade-off; and  $(50, 1.2, 0.14)$  for the grey dashed trade-off. Parameters for the critical functions are  $\mu = 1$ ,  $\rho(0) = 0.1$ , and  $\rho'(0) = 0.08$ .



**Fig. 7.** Bifurcations of monomorphic evolutionary singularities with trade-offs from the family in (14). Upper panels: one-parameter bifurcation plots. Thick continuous lines: convergence stable ESS; dashed lines: evolutionary branching points; dotted lines: evolutionary repellers. In (a), the fold bifurcation is between a branching point and a repeller, but the branching point turns into an ESS too close to the fold to show. In (b), note the short ESS segment at small values of  $b$ . Lower panels: two-parameter bifurcation plots of the convergence stable evolutionary singularity. Grey areas: no singularity exists (there is a fold bifurcation on the boundary of grey and white); black areas: the pathogen is not viable. Parameter values:  $\mu = 1$ ,  $\rho(0) = 0.1$ ,  $\rho'(0) = 0.08$ ; when not varied, the parameters of the trade-off are  $(a, b, c) = (50, 1.2, 1.5)$ . Note the different scale for  $a$  in the upper and lower panels.

function in (14) to obtain the singular point(s) numerically, and evaluated their evolutionary stability by calculating  $E$  in (6a). Convergence stability is easily deduced: Since  $\alpha = 0$  is not viable, there exists a minimum virulence,  $\alpha_{\min}$ , of viable strains, and  $\alpha_{\min}$  is evolutionarily repelling (Gyllenberg and Parvinen, 2001). It follows that the lowest monomorphic singularity is convergence stable, and if there is only one singular point, then it has convergence stability.

The one-parameter bifurcation plot with respect to  $a$  reveals that in a narrow range of  $a$ , two singularities exist within the virulence range shown in Fig. 7a (this is hard to see directly from Fig. 6 because both the critical functions and the trade-off are close to linear at the upper singularity). The upper singularity is a repeller, and evolutionary trajectories starting above this point lead to ever increasing virulence (recall from Fig. 6 that the trade-off is increasing steeper than the critical functions do near the border of viability); if the trade-off eventually saturates (not shown), then the trajectories will reach an attractor at some high

virulence. As expected, large values of  $a$  lead to evolutionary branching. When  $b$  increases (Fig. 7b), the singularity turns from an ESS into a branching point and then disappears via a fold bifurcation; for large  $b$ , virulence increases indefinitely as seen from Fig. 6. Increasing  $c$  leads to evolutionary branching and the position of the singularity becomes independent of  $c$  (Fig. 7c), again as expected from Fig. 6.

The two-parameter bifurcation plots in Fig. 7d–f indicate that evolutionary branching occurs in a large part of the parameter space. This is because the singularity often falls in the approximately linear part of the trade-off, and linearly increasing trade-offs lead to evolutionary branching when the critical functions are convex. Evolutionary branching is thus common within the family of trade-offs in (14), but not necessarily among other trade-offs. A classic few-parameter bifurcation analysis is always restricted to a given parameterized family of trade-offs, and may yield misleading results (for other examples, see de Mazancourt and Dieckmann, 2004; Geritz *et al.*, 2007).

The case of asymptotically constant trade-offs merits extra attention. With  $b = 0$  and finite  $c$ , the trade-off in (14) falls in Pugliese’s class of concave trade-offs that can only produce ESSs (Pugliese, 2002). As either  $a$  or  $c$  increases, however, the singularity approaches the ESS-branching point bifurcation (cf. Fig. 7d, f; see Fig. 5 for a similar singularity). With  $c \rightarrow \infty$ , the trade-off becomes a constant line, whereas with  $a \rightarrow \infty$ , the singularity shifts to high virulences where the trade-off has saturated to a constant line. With  $\beta$  constant, the only benefit from increased virulence is realized during superinfections, and is paid by the shortened lifetime of an infection. The singular strategy is exactly between an ESS and a branching point (with  $\beta' = \beta'' = 0$ , (6a) yields  $E = 0$ ), which supports co-existence whenever it is convergence stable and actually leads to evolutionary branching with any positive mutation size (see above).

## DISCUSSION

In this paper, we used critical function analysis to explore the possible evolutionary outcomes of a simple superinfection model (Adler and Mosquera-Losada, 2002; Pugliese, 2002) with three different modes of host population growth and under any conceivable trade-off function between transmission and virulence. Superinfections are known to facilitate the co-existence and evolutionary branching of pathogens (e.g. Adler and Mosquera-Losada, 2002; Boldin and Dieckmann, 2008). We find that evolutionary branching is indeed possible in a large part of the parameter space, provided that the local convexity of the trade-off falls within a certain interval. Too concave trade-offs result in ESSs, whereas too convex trade-offs result in evolutionary repellors. The convexity thus must pass between Scylla and Charybdis, in a range that is often limited (see Figs. 1–3), but includes at least some concave trade-offs as well (cf. inequality 6b). In contrast, the simple single-infection model of Andreasen and Pugliese (1995) may lead to evolutionary branching only with convex trade-offs (Pugliese, 2002; Svenningsson and Kisdi, in press).

It is noteworthy that evolutionary branching is possible even if  $\rho'(0) = 0$ , i.e. if higher virulence gives no advantage in superinfections. This possibility holds for constant population birth rate (Fig. 2c) or logistic growth (Fig. 3c), but not for constant population size (Fig. 1c) [the latter was assumed with constant  $\rho$  by Gandon *et al.* (2002)]. If  $\rho$  is constant at value  $\rho_0 > 0$ , the invasion fitness of a mutant strain simplifies from equation (3) into  $s_a(\alpha_{\text{mut}}) = \beta(\alpha_{\text{mut}})(\hat{S} + \rho_0 \hat{I}) - \rho_0 \beta(\alpha) \hat{I} - \alpha_{\text{mut}} - \mu$ , and the resident strain influences the invasion fitness of the mutant via two quantities,  $(\hat{S} + \rho_0 \hat{I})$  and  $\rho_0 \beta(\alpha) \hat{I}$  [recall that the

population dynamic equilibrium ( $\hat{S}$ ,  $\hat{I}$ ) depends on the resident]. With multiple resident strains  $i = 1, \dots, k$ , the invasion fitness is determined by two sums,

$$(\hat{S} + \rho_0 \sum_{i=1}^k \hat{I}_i) \quad \text{and} \quad \rho_0 \sum_{i=1}^k \beta(\alpha_i) \hat{I}_i$$

(cf. equations 1). This means that the model with constant  $\rho$  has only two environmental feedback variables, and hence can lead to the co-existence of at most two strains (Geritz *et al.*, 1997; Dieckmann and Metz, 2006; Meszena *et al.*, 2006; Durinx *et al.*, 2008) [for a detailed discussion of the role of environmental feedback variables in virulence evolution, see Svennungsen and Kisdi (in press)]. Evolutionary branching can happen once, yielding two co-existing strains, but further branching to higher levels of polymorphism is excluded. If  $\rho_0 = 0$  (superinfections never occur), the environmental feedback collapses to the single variable  $\hat{S}$ , and we recover an optimization model where  $\hat{S}$  is minimized (and  $R_0$  is maximized) by the optimal strain (Bremermann and Thieme, 1989; Dieckmann and Metz, 2006). Note that if  $\rho$  is not constant, then no analogous argument applies, and the number of environmental feedback variables does not constrain the potential number of co-existing strains.

If the transmission rate is constant and the only benefit of higher virulence comes from superinfections, then every evolutionary singularity is of the degenerate type between an ESS and an evolutionary branching point ( $E$  is zero in (6a)). There is a large area of mutual invasibility in the neighbourhood of a convergence stable singularity at the ESS–branching point bifurcation (Geritz *et al.*, 1998), and evolutionary trees will branch also at this degenerate singularity.

Another surprising feature of the model is mutual exclusion, which occurs under constant population size and logistic growth (Figs. 1 and 3) but not under constant population birth rate. Mutual exclusion (extinction of the rare strain whichever it is) is the opposite of co-existence by mutual invasibility. Since superinfections are known to support co-existence, the occurrence of mutual exclusion is unexpected. Mutual exclusion was observed by Mosquera and Adler (1998), but only when doubly infected hosts die instantaneously rather than clear one of the infections as our model in equations (1) assumes. Where mutual exclusion occurs, evolutionary branching is not possible with any trade-off.

As seen from the above discussion, the three different modes of host population dynamics yield contrasting results. Most studies of virulence evolution consider only one type of population dynamics and may not realize to which extent this choice affects the conclusions.

In this paper, we focused on monomorphic evolutionary singularities. It is possible to extend critical function analysis to find dimorphic singularities, evolutionarily stable coalitions of two strains or further evolutionary branching (Kisdi, 2006). The number of parameters, however, increases quickly: For the critical function analysis of monomorphic singularities, it is sufficient to specify the values of  $\rho(0)$  and  $\rho'(0)$ , but for the dimorphic case one needs the values and derivatives of the superinfection function at three separate points ( $\alpha_1 - \alpha_2$ , 0, and  $\alpha_2 - \alpha_1$ ; six parameters in total). A comprehensive analysis of dimorphic singularities is therefore much more demanding.

For the ease of analysis and following Pugliese (2002), we assumed that  $\rho(0) > 0$  and the superinfection function is everywhere differentiable. This is not the only biologically realistic choice, and different options may lead to qualitatively different evolutionary dynamics (Mosquera and Adler, 1998; Adler and Mosquera-Losada, 2002; Boldin and Diekmann, 2008). The

superinfection function is differentiable with  $\rho(0) > 0$  if the within-host dynamics of the competing strains is subject to demographic stochasticity. If the total number of pathogens within a host individual is a finite number  $N$  and a new infection with identical virulence enters the host with  $n$  pathogen particles, the old infection will be lost and the new infection goes to fixation with probability  $\rho(0) = n/N$ . In reality, however,  $N$  is so large that it may well be considered infinite, such that the existing infection is not subject to demographic stochasticity. On the other hand, a new infection of many diseases starts with a much smaller number of pathogens, such that demographic stochasticity plays a role in the initial phase of a new infection. In this case, the new infection undergoes a stochastic branching process within the host: A strain with higher virulence takes over the host with a positive probability, but a strain with lower virulence dies out with probability 1 (Jagers, 1975; Boldin and Diekmann, 2008). For small differences in virulence, the superinfection function has the form

$$\rho(\Delta\alpha) = \begin{cases} 0 & \text{for } \Delta\alpha \leq 0 \\ cn\Delta\alpha & \text{for } \Delta\alpha > 0 \end{cases}$$

[the ‘mechanistic’ case of Boldin and Diekmann (2008); see also Appendix B of Mosquera and Adler (1998)], i.e. it is not differentiable at zero. The present theory of adaptive dynamics (including critical function analysis) assumes differentiability, and the extension of the theory to non-differentiable functions is a future challenge motivated in particular by the non-differentiable superinfection functions arising naturally in virulence evolution models.

Note that with finite but large  $N$ , the superinfection function is close to the above non-differentiable form, with the value of  $\rho(0) = n/N$  close to zero but the function rising steeply at positive arguments. Because the derivative of such a superinfection function changes rapidly at zero (i.e.  $\rho''(0)$  is very large), the value of  $\rho'(0)$  is relevant only in the close vicinity of zero, and the analysis relying on  $\rho'(0)$  is valid only if the maximum size of mutations  $\Delta\alpha$  is sufficiently small such that  $\rho''(0)(\Delta\alpha)^2$  is negligible.

Note further that if  $n$  also goes to infinity such that the entire within-host dynamics is deterministic, then a new infection takes over the host if and only if it has higher virulence, i.e. we have the superinfection function

$$\rho(\Delta\alpha) = \begin{cases} 0 & \text{for } \Delta\alpha < 0 \\ 1 & \text{for } \Delta\alpha > 0 \end{cases},$$

which is discontinuous at zero [the ‘jump’ case of Boldin and Diekmann (2008)]. Such extreme asymmetry drives an evolutionary arms race to the maximum viable virulence (Mosquera and Adler, 1998; Adler and Mosquera-Losada, 2002; Boldin and Diekmann, 2008) and can maintain a continuum of different trait values in an evolutionarily stable population (Maynard Smith and Brown, 1986; Geritz, 1995; Adler and Mosquera, 2000), but the evolutionary dynamics of polymorphic populations under extreme asymmetry are not well understood.

#### ACKNOWLEDGEMENTS

This paper is dedicated to Tom Vincent to celebrate all his achievements and in particular his contribution to adaptive dynamics. Strangely enough, we never met, but ideas move easier than people. É.K. recalls the struggle to grasp the early papers on strategy dynamics, working as a student from the only

copy of the journal in a town behind the iron curtain, feeling quite lost among the equations but knowing that was the way to go. Those efforts have paid off nicely. Thank you, Tom.

The present research was supported financially by the University of Helsinki and by the Academy of Finland.

## REFERENCES

- Abrams, P.A. and Matsuda, H. 1994. The evolution of traits that determine ability in competitive contests. *Evol. Ecol.*, **8**: 667–686.
- Adler, F.R. and Mosquera, J. 2000. Is space necessary? Interference competition and limits to biodiversity. *Ecology*, **81**: 3226–3232.
- Adler, F.R. and Mosquera Losada, J. 2002. Super- and coinfection: filling the range. In *Adaptive Dynamics of Infectious Diseases: In Pursuit of Virulence Management* (U. Dieckman, J.A.J. Metz, W. Sabelis Maurice, and K. Sigmund, eds.), pp. 138–149. Cambridge: Cambridge University Press.
- Alizon, S. and van Baalen, M. 2005. Emergence of a convex trade-off between transmission and virulence. *Am. Nat.*, **165**: E155–E167.
- Andreasen, V. and Pugliese, A. 1995. Pathogen coexistence induced by density-dependent host mortality. *J. Theor. Biol.*, **177**: 159–165.
- Boldin, B. and Dieckmann, O. 2008. Superinfections can induce evolutionarily stable coexistence of pathogens. *J. Math. Biol.*, **56**: 635–672.
- Bowers, R.G., Hoyle, A., White, A. and Boots, M. 2005. The geometric theory of adaptive evolution: trade-off and invasion plots. *J. Theor. Biol.*, **233**: 363–377.
- Bremermann, H.J. and Thieme, H.R. 1989. A competitive-exclusion principle for pathogen virulence. *J. Math. Biol.*, **27**: 179–190.
- Castillo-Chavez, C. and Velasco-Hernandez, J.X. 1998. On the relationship between evolution of virulence and host demography. *J. Theor. Biol.*, **192**: 437–444.
- de Mazancourt, C. and Dieckmann, U. 2004. Trade-off geometries and frequency-dependent selection. *Am. Nat.*, **164**: 765–778.
- Dieckmann, U. and Metz, J.A.J. 2006. Surprising evolutionary predictions from enhanced ecological realism. *Theor. Popul. Biol.*, **69**: 263–281.
- Durinx, M., Metz, J.A.J. and Meszéna, G. 2008. Adaptive dynamics of physiologically structured population models. *J. Math. Biol.*, **56**: 673–742.
- Gandon, S., Van Baalen, M. and Jansen, V.A.A. 2002. The evolution of parasite virulence, superinfection, and host resistance. *Am. Nat.*, **159**: 658–669.
- Ganusov, V.V. and Antia, R. 2003. Trade-offs and the evolution of virulence of microparasites: do details matter? *Theor. Popul. Biol.*, **64**: 211–220.
- Geritz, S.A.H. 1995. Evolutionarily stable seed polymorphism and small-scale spatial variation in seedling density. *Am. Nat.*, **146**: 685–707.
- Geritz, S.A.H., Metz, J.A.J., Kisdi, É. and Meszéna, G. 1997. Dynamics of adaptation and evolutionary branching. *Phys. Rev. Lett.*, **78**: 2024–2027.
- Geritz, S.A.H., Kisdi, É., Meszéna, G. and Metz, J.A.J. 1998. Evolutionarily singular strategies and the adaptive growth and branching of the evolutionary tree. *Evol. Ecol.*, **12**: 35–57.
- Geritz, S.A.H., Van der Meijden, E. and Metz, J.A.J. 1999. Evolutionary dynamics of seed size and seedling competitive ability. *Theor. Popul. Biol.*, **55**: 324–343.
- Geritz, S.A.H., Kisdi, É. and Yan, P. 2007. Evolutionary branching and long-term coexistence of cycling predators: critical function analysis. *Theor. Popul. Biol.*, **71**: 424–435.
- Gilchrist, M.A. and Sasaki, A. 2002. Modeling host–parasite coevolution: a nested approach based on mechanistic models. *J. Theor. Biol.*, **218**: 289–308.
- Gyllenberg, M. and Parvinen, K. 2001. Necessary and sufficient conditions for evolutionary suicide. *Bull. Math. Biol.*, **63**: 981–993.

- Jagers, P. 1975. *Branching Processes with Biological Applications*. London: Wiley.
- Kisdi, É. 1999. Evolutionary branching under asymmetric competition. *J. Theor. Biol.*, **197**: 149–162.
- Kisdi, É. 2006. Trade-off geometries and the adaptive dynamics of two co-evolving species. *Evol. Ecol. Res.*, **8**: 959–973.
- Kisdi, É. and Geritz, S.A.H. 2001. Evolutionary disarmament in interspecific competition. *Proc. R. Soc. Lond. B*, **268**: 2589–2594.
- Levin, S. and Pimentel, D. 1981. Selection of intermediate rates of increase in parasite–host systems. *Am. Nat.*, **117**: 308–315.
- Levins, R. and Culver, D. 1971. Regional coexistence of species and competition between rare species. *Proc. Natl. Acad. Sci. USA*, **68**: 1246–1248.
- Matessi, C. and Pasquale, C.D. 1996. Long-term evolution of multilocus traits. *J. Math. Biol.*, **34**: 613–653.
- Matsuda, H. and Abrams, P.A. 1994. Runaway evolution to self-extinction under asymmetrical competition. *Evolution*, **48**: 1764–1772.
- May, R.M. and Nowak, M.A. 1994. Superinfection, metapopulation dynamics, and the evolution of diversity. *J. Theor. Biol.*, **170**: 95–114.
- Maynard Smith, J. and Brown, R.L. 1986. Competition and body size. *Theor. Popul. Biol.*, **30**: 166–179.
- Meszéna, G., Gyllenberg, M., Pásztor, L. and Metz, J.A.J. 2006. Competitive exclusion and limiting similarity: a unified theory. *Theor. Popul. Biol.*, **69**: 68–87.
- Metz, J.A.J., Nisbet, R.M. and Geritz, S.A.H. 1992. How should we define ‘fitness’ for general ecological scenarios? *Trends Ecol. Evol.*, **7**: 198–202.
- Mideo, N., Alizon, S. and Day, T. 2008. Linking within- and between-host dynamics in the evolutionary epidemiology of infectious diseases. *Trends Ecol. Evol.*, **23**: 511–517.
- Mosquera, J. and Adler, F.R. 1998. Evolution of virulence: a unified framework for coinfection and superinfection. *J. Theor. Biol.*, **195**: 293–313.
- Nee, S. and May, R.M. 1992. Dynamics of metapopulations – habitat destruction and competitive coexistence. *J. Anim. Ecol.*, **61**: 37–40.
- Nowak, M.A. and May, R.M. 1994. Superinfection and the evolution of parasite virulence. *Proc. R. Soc. Lond. B*, **255**: 81–89.
- Parker, G.A. 1983. Arms races in evolution – an ESS to the opponent-independent costs game. *J. Theor. Biol.*, **101**: 619–648.
- Pugliese, A. 2002. On the evolutionary coexistence of parasite strains. *Math. Biosci.*, **177/178**: 355–375.
- Svennungsen, T.O. and Kisdi, É. in press. Evolutionary branching of virulence in a single-infection model. *J. Theor. Biol.*
- Tilman, D. 1994. Competition and biodiversity in spatially structured habitats. *Ecology*, **75**: 2–16.
- Van Baalen, M. and Sabelis, M.W. 1995. The dynamics of multiple infection and the evolution of virulence. *Am. Nat.*, **146**: 881–910.

